HAL
open science

Evidence in the mouse for self-renewing stem cells in the formation of a segmented longitudinal structure, the myotome.

Jean Francois Daniel Nicolas, L Mathis, C Bonnerot, W. Saurin

To cite this version:

Jean Francois Daniel Nicolas, L Mathis, C Bonnerot, W. Saurin. Evidence in the mouse for self-renewing stem cells in the formation of a segmented longitudinal structure, the myotome.. Development (Cambridge, England), 1996, 122 (9), pp.2933-46. hal-01973671

HAL Id: hal-01973671

https://hal.science/hal-01973671v1

Submitted on 7 Aug 2019

HAL is a multi-disciplinary open access archive for the deposit and dissemination of scientific research documents, whether they are published or not. The documents may come from teaching and research institutions in France or abroad, or from public or private research centers.

L'archive ouverte pluridisciplinaire **HAL**, est destinée au dépôt et à la diffusion de documents scientifiques de niveau recherche, publiés ou non, émanant des établissements d'enseignement et de recherche français ou étrangers, des laboratoires publics ou privés.

Development 122, 2933-2946 (1996)
Printed in Great Britain © The Company of Biologists Limited 1996
DEV4664

Evidence in the mouse for self-renewing stem cells in the formation of a segmented longitudinal structure, the myotome

J. F. Nicolas*, L. Mathis and C. Bonnerot
With the contribution of **W. Saurin** for the statistical analysis

Unité de Biologie moléculaire du Développement, Institut Pasteur, 25 rue du Dr Roux, 75724 Paris Cedex 15, France

*Author for correspondence (e-mail: jfnicola@pasteur.fr)

SUMMARY

A novel method of clonal analysis has been used in the mouse to define the cellular events that lead to the formation of a segmented longitudinal structure, the myotome. Progenitor cells of the myotome were randomly marked during development by intragenic homologous recombination in transgenic mice expressing a reporter *laacZ* gene. 153 clones corresponding to 7829 cells, that is 20% of the myotomal population of one embryo, were obtained from 3000 E11.5 embryos. Their analysis leads to the hypothesis that, at E11.5, the 41 segments of the myotome have been mainly produced from a unique, spatially organised pool of self-renewing stem cells that accompanies the formation of the anterior-posterior axis.

Key words: anterior-posterior axis, asymmetric fate, cell lineage, clonal analysis, mouse embryo, *laacZ*, paraxial mesoderm, somite

INTRODUCTION

Perhaps the most crucial aspect in the development of vertebrates is the formation of the longitudinal axis of the embryo during gastrulation. The axis is subsequently organised into metameric units corresponding to the somites in the paraxial mesoderm (Tam and Beddington, 1987; Keynes and Stern, 1988; Christ and Ordahl, 1995) and to the neuromeres in the central nervous system (Lumsden and Keynes, 1989; Puelles and Rubenstein, 1993). Superimposed on the formation of the axis is a corresponding longitudinal organisation of gene expression patterns involved in the progressive specification of cell fates (Kessel and Gruss, 1990; McGinnis and Krumlauf, 1992; Slack et al., 1993; Burke et al., 1995). The temporal overlap of axis formation and the expression of particular developmental genes suggest an interrelation between the spatiotemporal distribution of cells and the sequential activation of developmental genes. To elucidate the nature of this interrelation, it is necessary to better understand cell behaviour during axis formation, namely, the rules of cell proliferation and distribution.

Different models of axial structure formation in vertebrates have been proposed, and it is possible to envisage four principal representative models whose main features are schematically presented in Fig. 1. In one model, axis formation results from mechanisms involving convergence, elongation and cell intercalation during gastrulation (Fig. 1A). In this model, there is neither early regionalization nor temporal distribution of the precursors. Patterns obtained from labelled cells in *Xenopus laevis* have been interpreted as showing that mediolateral cell intercalation occurs in the dorsal mesoderm since this region underlies convergent extension and differentiates into somites and notochord (Keller and Danilchik, 1988; Keller and Tibbetts, 1989). Similar cell movements in Zebrafish during epiboly and gastrulation, as well as during formation of central nervous system, have also been interpreted as mediolateral cell intercalation and convergent extension (Kimmel et al., 1994). In a second model, an early (i.e., before axis formation) regionalisation of precursors is postulated (Fig. 1B), for instance, the neural axis of mammals is postulated to form longitudinally from precursors already organised in a craniocaudal pattern in the epiblast (before gastrulation). Descendants of cells from the distal part of the epiblast would distribute at the late primitive streak stage in relation to their initial anteroposterior position (Quinlan et al., 1995). This model could also be applied to axial and paraxial mesoderm which would also be regionalized. In a third model, there is a temporal distribution of the precursors whose descendants are sequentially allocated to the axis. This latter model has been proposed for the formation of axial and paraxial mesoderm in the mouse (Tam and Beddington, 1987; Tam and Trainor, 1994) and chick (Stern et al., 1992). This model has two distinct aspects depending on whether the pool of precursors is changing (rapid recruitment and loss of new cells, Fig. 1C) or permanent (self-renewing cells, Fig. 1D). Selleck and Stern (1992) have proposed that Hensen's node contains stem-cell-like cells that can give rise to notochord and stem-cell-like cells that eventually give rise to medial somites. In these latter models, if the pool of precursors is changing, the mode of formation is both regional and temporal but if the pool is permanent, the mode of formation is essentially temporal.

These models have been based on the analysis of the descendants of individual cells or of groups of cells traced by fluorescent labelling. So far, none of these models has been formally established nor can they be considered to be exclusive of one another. The incomplete understanding of such a fun-

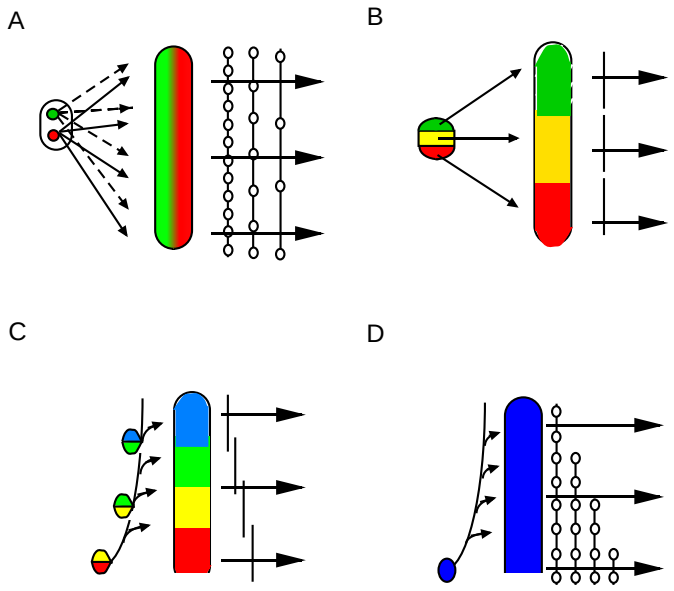

Fig. 1. Models of formation of a longitudinal structure. Four possible models of formation of a longitudinal structure represented in relation to its pool of precursor cells. (A) Extension and intercalation; (B) early regionalization; (C) temporal production of the precursors from a changing pool of cells and (D) temporal production from a unique self-renewing pool of cells. On the left is a representation of the pool of precursor cells at an early stage and in the middle a representation of the longitudinal axis after its formation. Shown on the right side of each figure are the longest clones expected from the labelling of a cell in the pool of precursors. The horizontal arrows represent clonal complexity (see text) in relation to axial level.

damental problem is perhaps due to the inherent difficulties in performing a complete lineage analysis in vivo, and this applies particularly to mammals. Beside the difficulties associated with techniques of cell labelling and in vitro culture of mammalian embryos, which can be partly overcome during short term analysis (Rossant, 1987; Beddington and Lawson, 1990), there is the greater obstacle of recognising whether the most representative cells have been traced. In this regard, clonal analysis using prospective methods are not objective because the site and time chosen for cell labelling are arbitrary. Non-clonal analyses, using a group of labelled cells, give information about the global distribution of cells, but do not delineate the genealogical relationships between the descendants of the labelled cells.

We have re-examined the mechanisms involved in the formation of a longitudinal structure in the mouse using a new retrospective clonal approach that overcomes many of the difficulties described above. Cell clones are labelled in embryos by a random genetic event in a *lacZ* reporter gene (Bonnerot and Nicolas, 1993b). This reporter construct (Bonnerot et al., 1987) contains an internal duplication of the *nls lacZ* gene (*laacZ*) that inactivates β-galactosidase activity. If an intragenic homologous recombination occurs between the duplicated sequences of the *laacZ* (β-gal$^-$) transgene, it reestablishes the *lacZ* (β-gal$^+$) reading frame and results in functional β-gal expression. This can happen in all cells and at any time during development. The probability of generating a clone, at any given time, is dependent on the number of precursor cells that give rise to the structure examined. Consequently, this retrospective clonal approach allows for a determination of the time at which precursors of the structure were organised into a 'coherent' pool of cells (predictable origin). The recombination event in the *lacZ* reporter gene

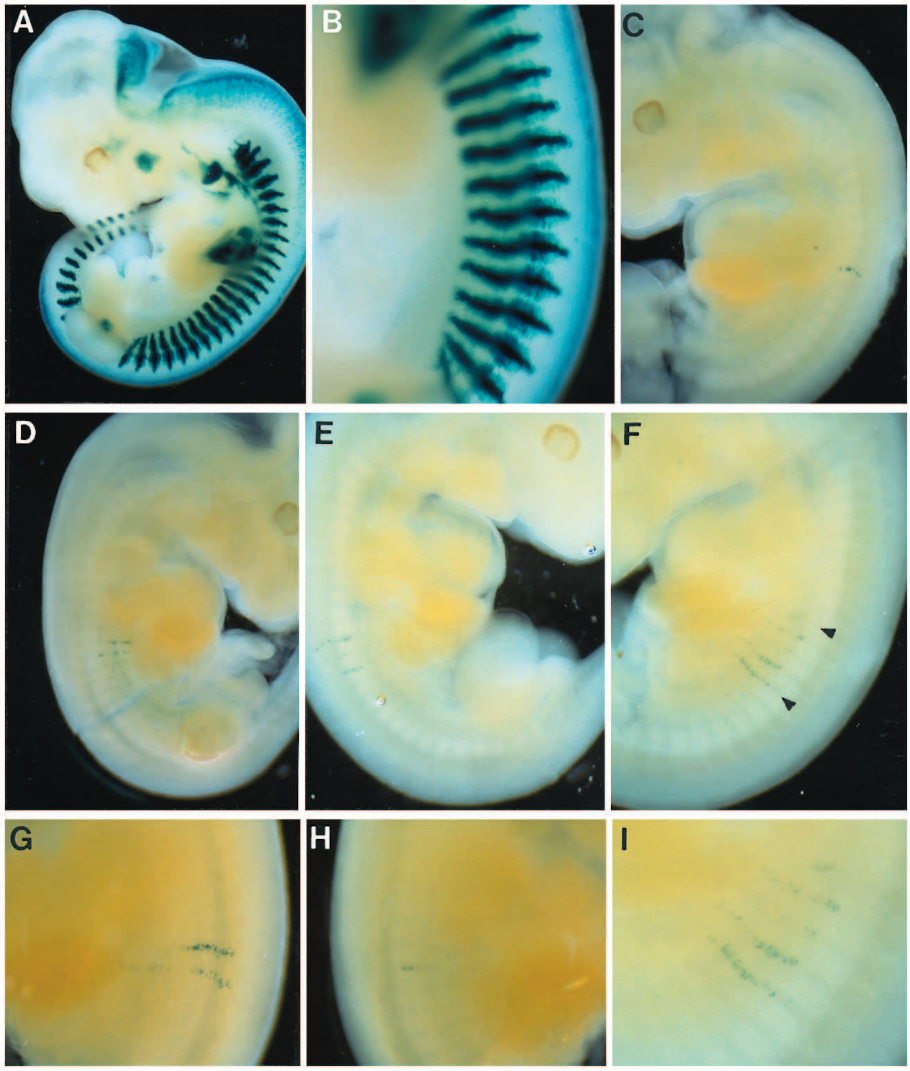

Fig. 2A-I

generates an intrinsic long-term marker (β-galactosidase) that allows visualisation of the descendants of the ancestral cell (Sanes et al., 1986; Bonnerot and Nicolas, 1993a) even in a mature differentiated structure and should permit an analysis of all cells at the origin of this structure (Bonnerot and Nicolas, 1993b). This method has been applied to the study of the myotome, a structure derived from the paraxial mesoderm and which is organised at embryonic day 11.5 (E11.5) into 37 to 42 individual segments along the A-P axis corresponding to the dorsal part of the somites (Christ and Ordahl, 1995).

MATERIALS AND METHODS

Stocks of transgenic animals were maintained by intercrosses. Mice homozygous for the transgene were detected by PCR analysis of the progenies derived from crosses between C57BL/6XDBA/2 non-transgenic F_1 animals, as described (Bonnerot and Nicolas, 1993a). The β-gal$^+$ clones were obtained from 10 males of one transgenic αAChRnl-slaacZ line (α 2) harbouring two copies of the transgene (Bonnerot and Nicolas, 1993b). We searched for the presence of cells with a recombinant *lacZ* transgene by examination of E11.5 X-gal-stained embryos derived from females (C57BL/6XDBA/2) crossed with homozygous *laacZ* males. The morning when copulation plugs were found was taken as 0.3 days p.c. (E0.3). In situ staining or whole-mount X-gal staining was performed as previously described (Bonnerot et al., 1990). The serial number of the myotomal segments containing β-galactosidase-positive cells was recorded in comparison with X-gal-stained embryos from RαNLZ2, a transgenic line harbouring a αAChRnlslacZ transgene (Klarsfeld et al., 1991). The enumeration of the β-gal$^+$ cells within each segment was done by direct observation using a stereomicroscope model. For the counting of β-gal$^+$ cells in the RαNLZ2 control embryo, each segment was first dissected and slightly crushed under a coverslip and then enumerated at ×400 with a microscope.

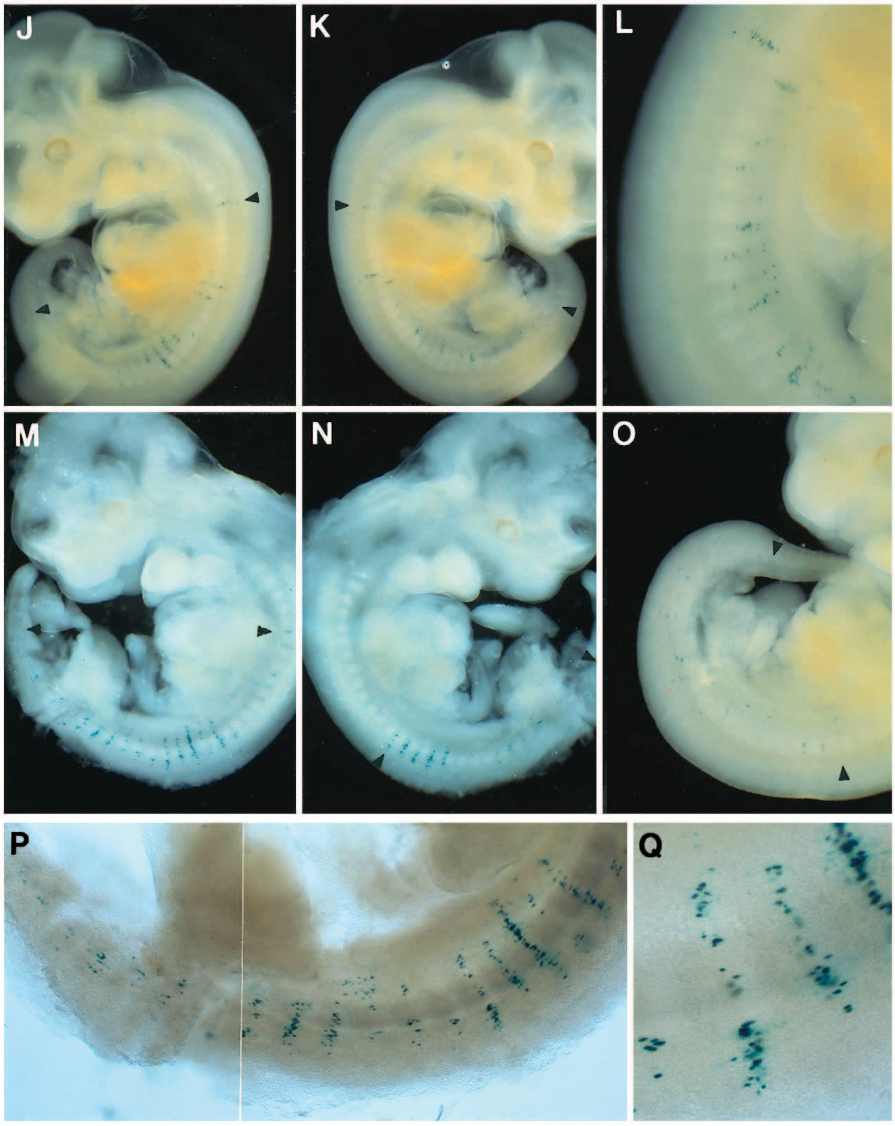

Fig. 2J-Q

Fig. 2. Examples of recombinant *lacZ* clones. In situ whole-mount X-gal staining of E11.5 embryos. (A) β-gal-staining pattern in a transgenic RαNLZ2 E11.5 embryo; (B) same embryo at higher magnification. The myotome is organised into 37-42 segments containing mononucleated differentiated muscle cells. The forelimb is in regard to segment 7 to 11 and the hindlimb is in regard to segment 25-29. (C-I) Examples of short clones; (J-Q) Examples of long clones. (C) A monosegmented, unilateral clone with longitudinal extension (L value) of 1. Clone SC 37 has 32 β-gal$^+$ cells which are all clustered in the eleventh, segment on the left side of the embryonic axis (Sa=11). (D) A bisegmented, unilateral clone of L=2. SC1 has 50 β-gal$^+$ cells distributed into segments 14 and 15 on the right side of the embryo. (E) A bilateral clone of L=6. Clone SC37 has 73 β-gal$^+$ cells clustered in the 14/16 right segments (arrow heads) and in the 18/19 left segments (not represented); Sa=14, Sp=19. This is an example (6 cases out of 30) of imperfect left-right asymmetry. (F) A unilateral clone of L=5. Clone VG8 has 114 β-gal$^+$ cells clustered in five adjacent segments number 12/16 on the left side of the embryo. Sa=12, Sp=16. (G,H) A bilateral clone of L=4. Clone VG3 has 156 β-gal$^+$ cells distributed in the 15-16 left segments (70 and 65 cells) and 14-17 right segments (4, 16, 0 and 1 cells). Sa=14, Sp=17. (I) Higher magnification of clone VG8; segments 12-16 with 12, 26, 6, 36 and 34 β-gal$^+$ cells respectively. (J-L) Clone VG70 has 498 β-gal$^+$ cells distributed into 37 segments from the left (J) and right (K) side of the embryo. Arrow heads indicate Sa and Sp positions of the clone. Its L value is 29. (L) Higher magnification of the right side of the clone from segment 11-25. (M,N,P,Q) Clone SC67 has 727 β-gal$^+$ cells distributed into 40 segments from the left (M) and right (N) side of the embryo. Arrowheads indicate Sa and Sp positions of the clone. (P) Higher magnification of the left side of the clone from segment 15-33. (Q) Detail of segments 18-21 with 55, 37, 57 and 7 β-gal$^+$ cells respectively. (O) Clone SC9 extends from segment 15-37 (arrowheads). It has 173 β-gal$^+$ cells and a L value of 23.

RESULTS

Production of embryos exhibiting β-gal$^+$ clones

A transgenic mouse harbouring a *lacZ* reporter gene that had been inactivated by an internal duplication (*laacZ*) was produced as previously described (Bonnerot and Nicolas, 1993b). In order to analyse the lineage of cells in the myotome, the expression of the *laacZ* gene was driven by the promoter of the α subunit of the acetylcholine receptor (αAChR), which limits expression specifically to cells of this compartment (Klarsfeld et al., 1991; Sanes et al., 1991). The β-gal$^+$/β-gal$^-$ mosaicism in somatic cells is initiated in transgenic embryos by a homologous recombination event between the duplicated sequences in *laacZ*, which re-establishes the open reading frame for the reporter gene. The frequency of E11.5 embryos exhibiting β-gal$^+$ cells was 153 of 3000, or about one out of twenty embryos. This low frequency verifies that most of the positive embryos contained only β-gal$^+$ cells from a single recombinant clone, because the probability of more than one recombination events occuring in cells of the myotome of the same embryo is $1/20^2$. The results presented below represent analyses of 153 positive β-gal$^+$ embryos, corresponding to the labelling of 754 segments and 7829 β-gal$^+$ cells.

In the 40-45 somites of the control RαNLZ2 transgenic embryos (E11.5) the entire myotomal compartment was composed of 32000-44000 β-gal$^+$ cells distributed into 37-42 segments, as estimated by direct enumeration. In the E11.5 embryo, the β-gal$^+$ labelling was not very extensive in the limb buds, therefore clones including cells from these structures will not be discussed further. The 153 clones analysed represent a sample comprising about 18 to 24% of the myotome of one embryo. Other considerations (see Discussion) indicate that this number of clones closely approximates saturation, in that none of the newly produced clones had geometric characteristics different from the clones already obtained. Therefore we assume that some rules of myotome formation can be ascertained by analysing this sample of clones further.

Cell arrangement in β-gal$^+$ clones in E11.5 embryos

Clones were assessed by three main parameters: their cell number, the position of the most rostral segment to which they contributed, (that is, their anterior border, Sa) and the portion of the axis to which they contributed, indicated by their longitudinal extension (L) and expressed as number of segments.

A few consistent features of cell arrangement in the clones clearly emerged (Fig. 2). First, there were clones that contributed to only a small number of segments (Fig. 2C-H). For these short clones, regardless of the number of labelled segments, the number of β-gal$^+$ cells per segment was invariably low compared to the total number of myotomal cells per segment (Fig. 2, compare B and I). A few of these short clones contributed to segments on both sides of the myotome (Fig. 2E,G,H). In these cases, the left and right participation is almost always (24 cases) at identical axial levels or at most shifted by only one segment (6 cases). Apart from the coherent group of labelled segments, β-gal$^+$ cells were never observed rostrally or caudally. This indicates that cells that are genealogically related are also geometrically close. A second set of clones contributed to a large number of segments (Fig. 2J-P). Certains ones started in the most anterior segments and continued posteriorly (Fig. 2J,K,M), whereas others started more caudally but still continued posteriorly (Fig. 2O). For these long clones, the number of β-gal$^+$ cells per segment was always low in comparison with the total number of myotomal cells per segment (Fig. 2, compare B and Q). This number was comparable to the contribution of β-gal$^+$ cells to short clones (Fig. 2, compare I and Q). These long clones also contributed frequently to segments on both sides of the myotome (Fig. 2J,K and M,N).

Axial position of the clones

A classification of the 153 clones according to their anterior border (Sa) is presented in Fig. 3A. This classification reveals important information about the geometric positions of the clones.

First, there were several long clones (indicated by filled bars in the figure) which participated in a significant portion of the axis. The four clones with the highest L value (32 to 40) contributed to the myotome from segments 2 to 41 (Fig. 3A, left part). These clones demonstrated a common clonal origin (i.e. common precursors) for at least a fraction of the cells in these segments.

Second, almost all long clones extend caudally a long distance from their anterior border. This point is made more clearly when individual long clones are grouped together (Fig. 4A), and is demonstrated quantitatively and statistically as follows: (a) by calculating the number of long clones participating in a segment at each axial level (Fig. 4B): the distribution is not uniform, there were more long clones contributing to posterior segments than to anterior segments and (b) by measuring the longitudinal extension of long clones at each axial level (Fig. 4C): their L value tend to be maximum in relation to the axial position of their anterior border and therefore the smaller clones positioned more posteriorly. It should be noticed that the distributions in Fig. 4B,C give a partially inaccurate picture of these points because certain clones have an under-estimated L value due to an incomplete maturation of the more caudal part of the myotome at E11.5 (data not shown). It is also for this reason that certain aspects of this analysis concern only the first 30 segments. Nonetheless data shown in Fig. 4A-C indicate that the category of long clones is polarised from anterior to posterior. If we consider clonal complexity to be the number of times a segment is labelled by a clone, then clonal complexity increases from rostral to caudal when considering long clones.

Third, short clones constitute a second category of clones (indicated by grey boxes in Fig. 3A). For the 122 short clones analysed, their L value was less than 7 segments long, and their contribution to posterior or anterior segments is unlikely to be not uniform (Fig. 5A,B). In other words, clonal complexity of individual segment does not significantly increase from rostral to caudal when considering clones with an L value <7. Again it is important to note the decrease in the number of short clones for those segments posterior to segment 30 (Fig. 5B), due to an incomplete maturation of the more caudal part of the myotome.

Numeric relationship between long clones

The random generation of the clones implies that the frequency of clones representing each L value is proportional to the number of precursors at their origin. The L values for the long clones described in Fig. 4A were from 7 to 40, and the frequency of long clones in relation to their L value did not

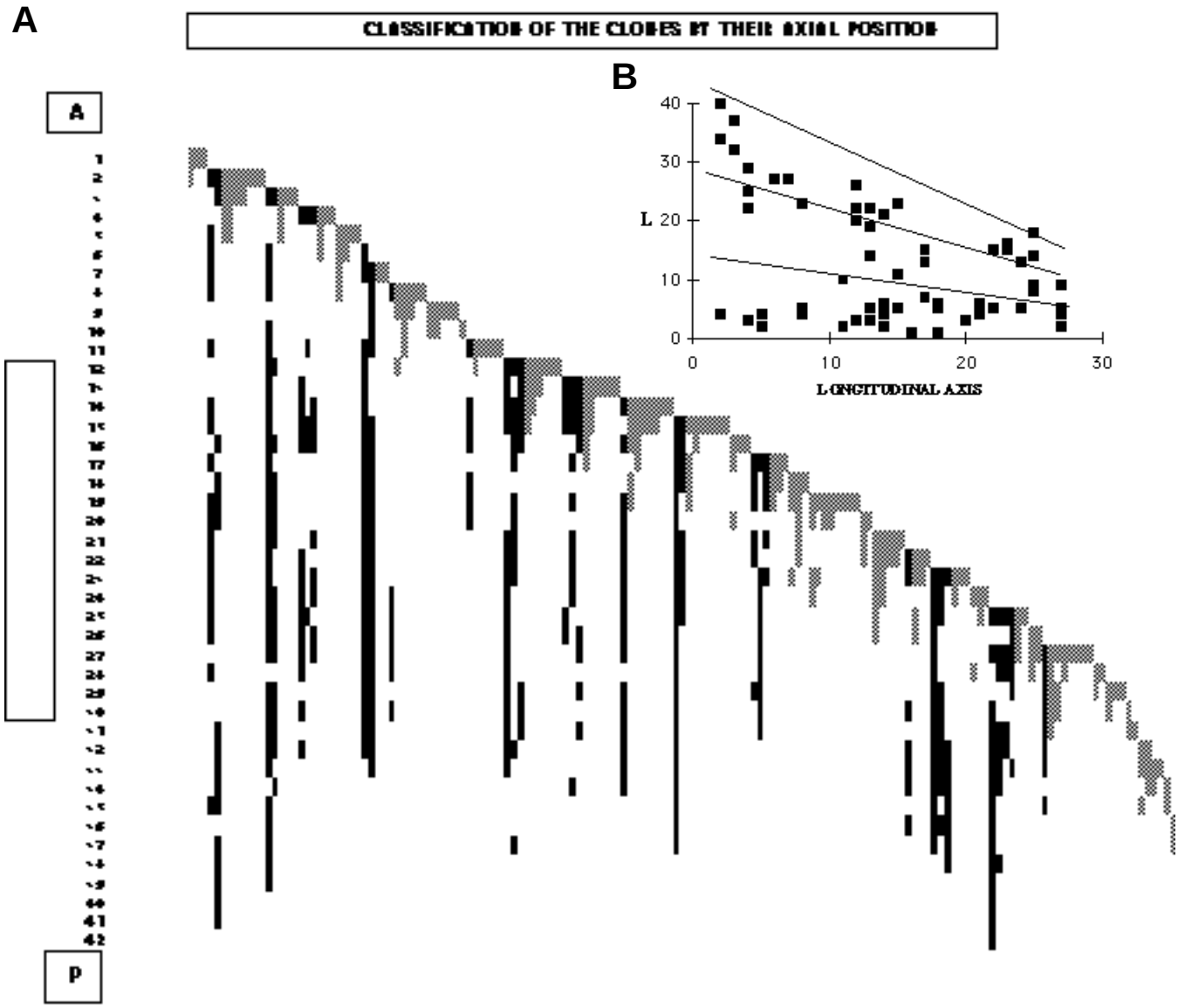

Fig. 3. Classification of the clones according to the most anterior segment to which they contribute. (A) Clones 1 to 153 (x axis) were ordered according to the most anterior segment (SA) to which they contributed (y axis). The L>6 clones are indicated in dark and the L≤6 clones in grey. (A) Anterior and (P) posterior level of the embryos. (B) L values (y axis 0 to 40) of the long and short bilateral clones (x axis) ordered according to their SA value. To test whether bilateral clones could have any L value between the maximum possible value (L max) and 1, a graph representing L values in relation to axial level has been divided into three domains of equal probability of 1/3 (B). There are 18, 12 and 28 clones in the domain of long, medium and short clones respectively. For these values, χ^2 testing of the uniformity of repartition is equal to 6.76 (2 d*f*), *P*=0.034. Therefore, we consider that uniformity is unlikely and that there are two main categories of bilateral clones. Fig. 3A further suggests that the cut-off value between long and short clones is at L=6-7.

vary significantly (Fig. 6A, L7 to 40). Moreover, the probability of generating a long clone as defined by its Sa value, did not change in relation to the longitudinal axis (Fig. 6B), since a statistical analysis (see the legend of Fig. 6) showed that the frequency of long clones for segments 1 to 10, compared to the frequency for segments 11 to 20 and/or 21 to 30, did not differ. These data suggest that these long clones were produced from precursors pools of similar sizes.

If we then suppose that long clones having different L values can be genealogically related, then the number of β-gal$^+$ cells in individual clones can provide information about their relationship to their precursors. If the pool of long clones generated and maintained their pool of precursors through a symmetrical (proliferative) mode, then the frequency of clones of a given size (measured as β-gal$^+$ cells), grouped by exponentially increasing sizes (e.g. 1, 2, 3-4, 5-8, 9-16, etc.), would decrease exponentially (1/2, 1/4, 1/8, 1/16, 1/32) (see the inset a′ in Fig. 7). In contrast, if precursors were maintained by an asymmetrical (stem cell) mode, in which one of the two daughter cell has a limited contribution to the myotome, the frequency of clones would increase exponentially (see the inset a″ in Fig. 7). The observed distribution of the sizes for long clones suggests that the mode of maintenance for the pool of common precursors does not follow a symmetrical mode; rather, it is

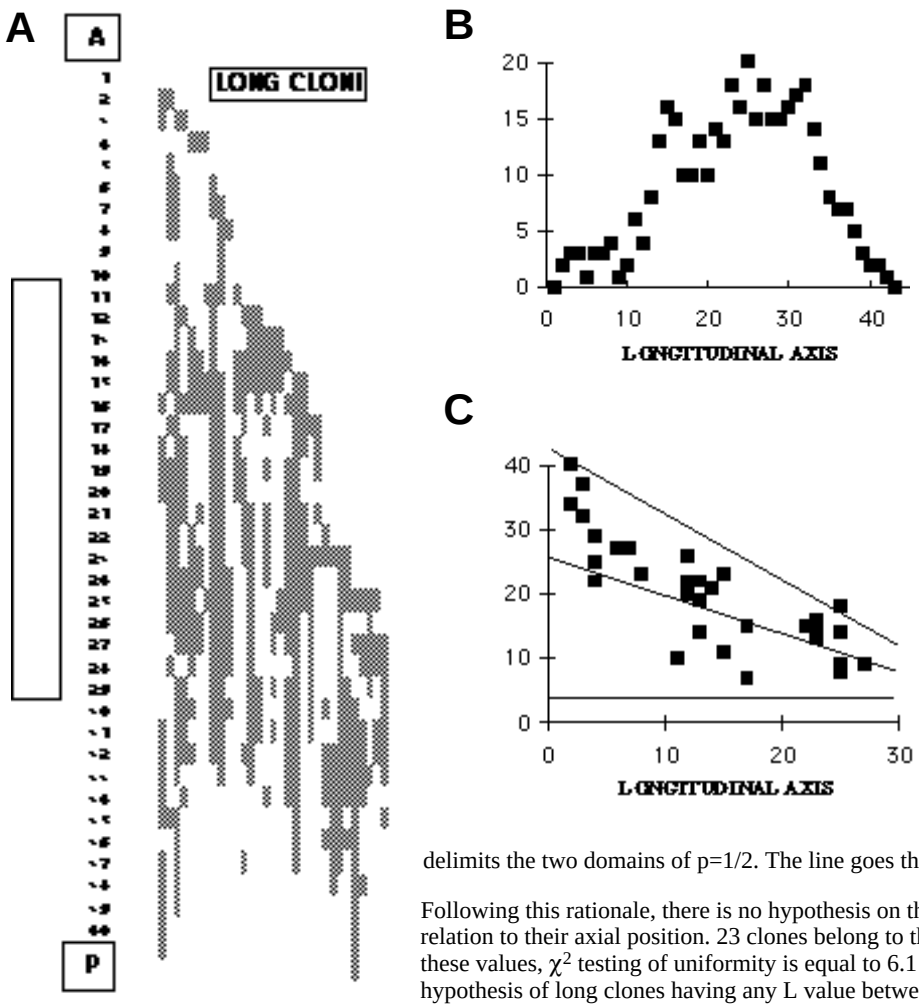

Fig. 4. Long clones: increased rostrocaudal clonal complexity. (A) The 32 long clones (x axis) were ordered according to the most anterior segment to which they contributed (y axis). A, anterior and P, posterior level of the embryos. (B) Clonal complexity. Number of times (y axis) a segment (1 to 42, longitudinal axis) is labelled by long clones. We have tested the non uniformity in the number of times a segment is labelled for the first 30 segments. 15 coupled values, representing two successive segments, have been compared. For long clones, χ^2=245.1 (14 df); $P<10^{-6}$, therefore we consider that their distribution is not uniform. (C) L values of long clones (y axis) in relation to their most anterior axial level (x axis). Test of distribution of the clones between the two domains of equal probability indicates non uniformity ($P<10^{-3}$). Statistical test. To test if the long clones could have any L value between the maximum (Lmax) possible value and L=7, the graph has been divided into two domains of equal probability. The horizontal line at L=6 delimits the excluded domain of clones having L<6. The upper transverse line delimits the domain of all other possible L values and the second transverse line delimits the two domains of p=1/2. The line goes through the points $\left[\frac{\text{Lmax-6}}{2}\right]$.

Following this rationale, there is no hypothesis on the individual probabilities of the clones in relation to their axial position. 23 clones belong to the upper domain and 9 to the other domain. For these values, χ^2 testing of uniformity is equal to 6.1 (1 df), P=0.013. Therefore, we reject the hypothesis of long clones having any L value between Lmax and L=7.

closer to an asymmetric mode, in which cells of the precursor pool generate daughter cells with identical properties (self renewing) and cells with a more limited myotomal potential.

Bilateral location of the clones

A frequent characteristic of the long clones was their bilateral location (Table 1). 90% of the long clones participated in the development of both left and right sides of the myotome. This characteristic was observed all along the axis when individual clones were examined (data not shown). There were however some long clones that were strictly unilateral. Similarly, 80% of the short clones with an L value of 4 to 6 also contributed to both sides of the myotome. This bilateral location was observed at all axial levels from rostral to caudal. The frequency of bilateral clones decreased rapidly in the L 3 to L 1 categories; therefore, there appears to be a transition in the bilateral distribution of descendants of clones having an L value of >3 and clones having an L value of <3, although we still observed two bilateral clones with an L value of 1.

Further characteristics of the pattern of clones

The production of long clones may correspond to the production of genealogically related short clones having L values ≤ 6

Table 1 indicates that precursor cells of most short clones having L values of 4 to 6 (and some clones with L<4) share the same capability to contribute to segments on both sides of the embryo as precursor cells for long clones. This suggests that their precursors are spatially located in a structure that

Table 1. Bilaterality of the clones

Clone extension	Number of clones	Percent of bilateral clones	Position of the bilateral segments	
			A	P
7 to 40	30	90	4	36
6	5	80	14*	26*
5	9	80	8*	31*
4	9	80	2	35
3	9	40	4	22
2	26	20	5	35
1	33	10	16	28

Clonal extension: L value of the clones.
Number of clones: total number of clones in each class.
Fraction of bilateral clones: number of bilateral clones divided by total number of clones in each class.
Position of the bilateral segment: A refers to the most anterior segment showing bilateral contribution. P refers to the most caudal segment showing bilateral contribution.
* indicates that the segment is also the most anterior (or posterior) segment of the clones of the group considered.

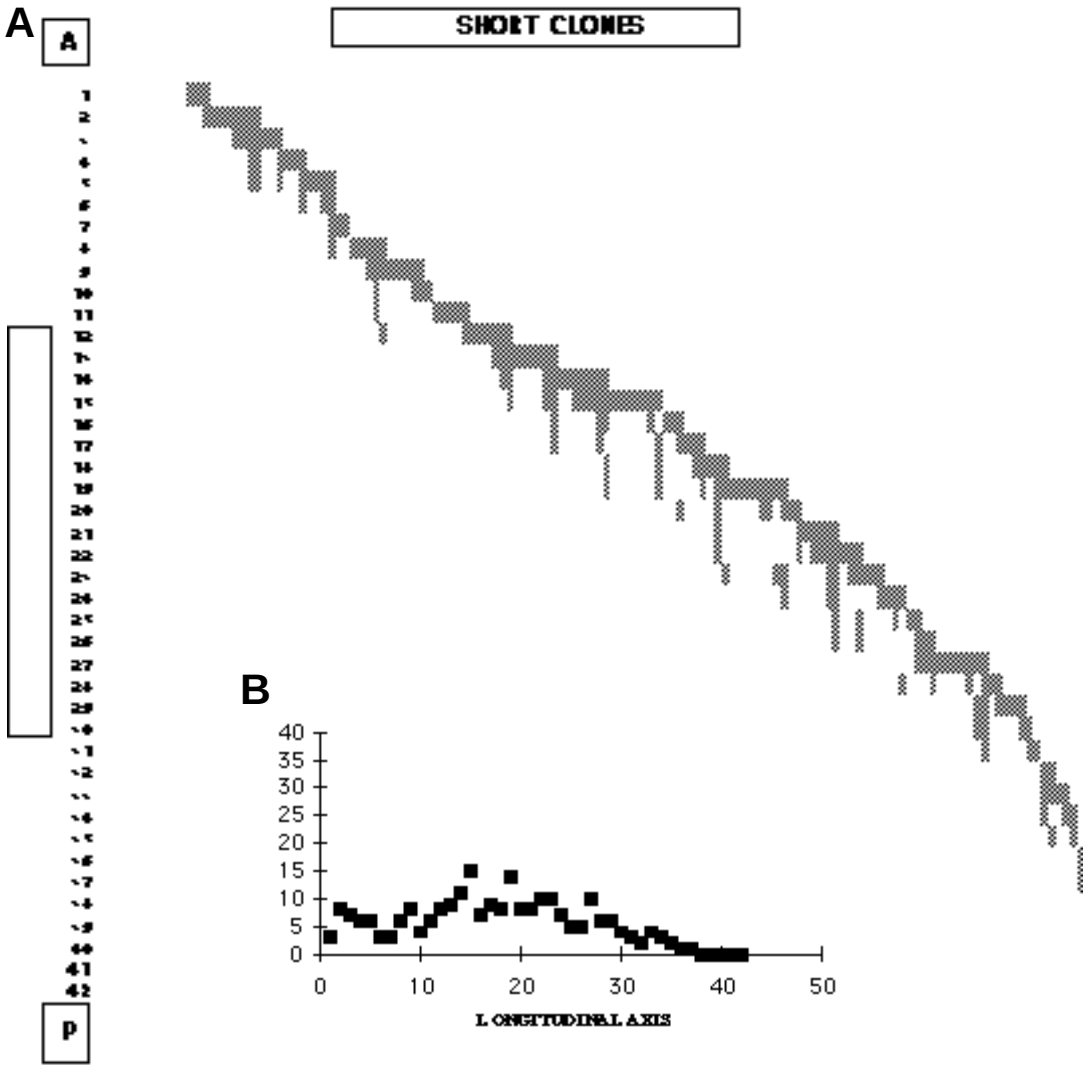

Fig. 5. Short clones: uniform rostrocaudal clonal complexity. (A) The 122 short clones (x axis) were ordered according to the most anterior segment to which they contribute (y axis). A, anterior and P, posterior level of the embryos. (B) Clonal complexity: number of times (y axis) a segment (1 to 42, longitudinal axis) is labelled by short clones. Statistical test: we have tested the non uniformity in the number of times a segment is labelled for the first 30 segments. 15 coupled values representing two successive segments, have been compared. χ^2=21.1 (14 df); $P=10^{-1}$. Therefore, we consider it unlikely that their distribution is not uniform.

includes left and right segments. Therefore, precursor cells for long and short bilateral clones might be genealogically related.

Additional arguments for a genealogical link between long and short bilateral clones follow. (a) If short bilateral clones derived from a pool of precursor common with long clones, their frequency should be equal. Indeed, the frequency of L>6 clones (32/153) is close to the frequency of short bilateral clones (30/153). (b) The hypothesis of a common origin implies that a long clone would correspond to several short clones and that the mean contribution of these two classes of clones to the formation of each segment should therefore be equal. Table 2 summarises the average segmental contribution of the classes of clones. The values (13.6±0.84 and 15.2±1.94) are not statistically different and thus support the hypothesis.

These pieces of data – bilaterality, frequencies and average segmental contribution – fit with the hypothesis that long clones share a common pool of precursor cells with short clones. If this is true, it demonstrates that cells segregated by

Table 2. Average segmental contribution by short bilateral and long clones

Clone	Total number of clones	Total number of cells	Total number of segments	Segmental contribution
Long	32	5171	379	13.6±0.84
Short bilateral	30	1464	96	15.2±1.94

Mean of the contribution of clones (in β-gal$^+$ cell number) by segment.
Number of clones: total number of clones in each class.
Number of cells: total number of β-gal$^+$ cells for all clones of each class.
Number of segments: total number of segments to which the clones of each class contributed (each segment corresponds to the right + the left segment).
Average segmental contribution: number of cells divided by number of segments.
Statistical test: we have tested whether the mean contribution of long clones per segment (379 values) is different from the mean contribution of short bilateral clones per segment (96 values): u=0.82 (ns); therefore, the contributions are not statistically different.

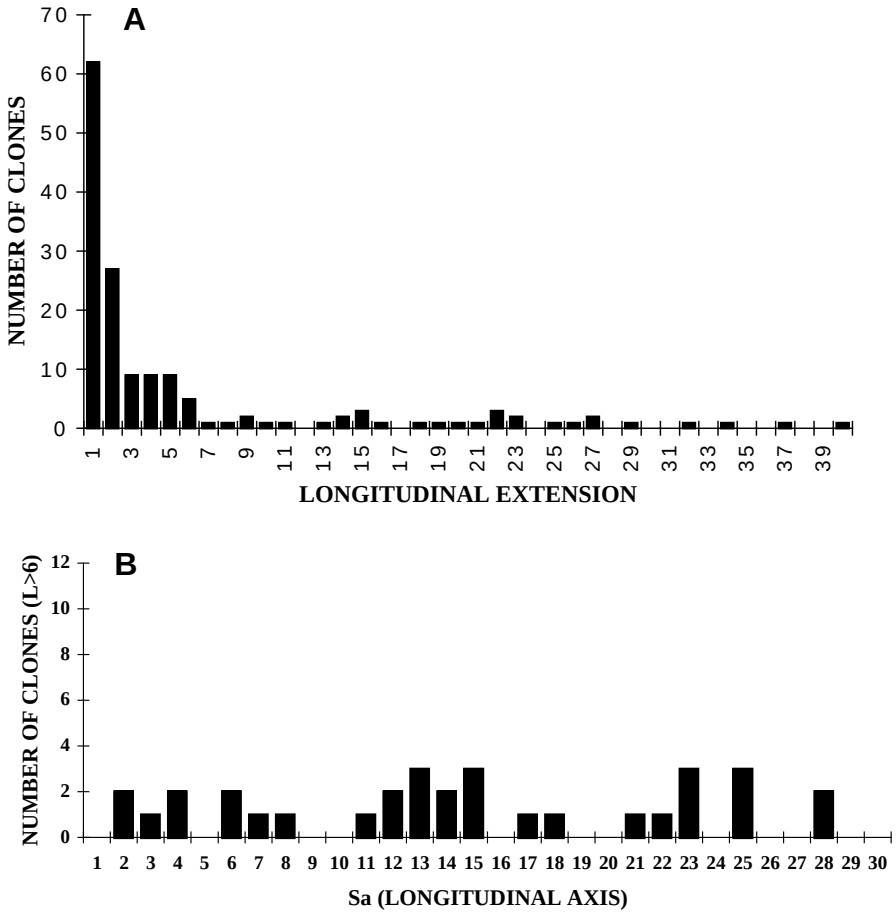

Fig. 6. (A) Number of clones of a given L value. x axis represents L value of the clones (from 1 to 40), y axis represents the number of clones. (B)Number of long clones (L>6) of a given Sa value. x axis represents number of long clones. y axis represents their Sa value (longitudinal axis from segments 1 to 30). Statistical test: we have examined whether the frequency of long clones having Sa values between 1 to 10 (9/32) is different from the frequency of long clone having Sa values between 11 to 20 (13/32), and 21 to 30 (10/32). χ^2=1.032, (2 df), *P*=0.59. Therefore we consider that the distribution of clones in these three groups is uniform.

the pools of precursors of long clones have a heterogeneous longitudinal property. In particular, the number of segments to which they contribute may vary from 6 to 1.

Numerical relationship between long and short clones

Following further the hypothesis that a common pool of precursors exists for long and short bilateral clones, then the contribution of this pool to both these classes implies that, on average, for each long clone there is a single corresponding short clone. Therefore, an increasing rostrocaudal overrepresentation of long clones versus short bilateral clones in the myotome is expected (see the inset in Fig. 8). This is, in fact, observed: the ratio of the number of long clones contributing to a given segment to the number of short bilateral increases rostrocaudally. The slope of the curve suggests that on average one short clone is produced every 4-5 segments indicating that, on average, a long clone contributing to the whole axis (L=36) corresponds to 8-9 short clones. It is important to note that this calculation does not indicate a regularity in the production of small clones from an individual precursor of long clones. For instance, it does not indicate whether the small clones produced from the same precursor overlap or not. Further analysis of the longitudinal organisation (periodic distribution along the axis) of long clones may help address this point.

Size of the pool of precursor

From the numerical data, it is possible to approximate the size of the pool of self-renewing precursors that form the myotome. If the pool of precursors derived from equivalent cells, its size could be estimated from the fraction of the myotome contributed by a long clone. This calculation gives a pool size of

Table 3. Size of the pool of precursor cells

	Long clones (segments 1 to 30)	Short bilateral clones (segments 6 to 30)
Polyclonal size	137±18	152±22

The number of precursors necessary to produce the whole myotome (polyclone size) has been calculated from the number of β-gal$^+$ cells in the long and short bilateral clones. We determined precursor cell number using the descendant clone size estimation method, an adaptation to our system of the minimum descendant clone size estimation method of Rossant (1984). For long clones, the total number of β-gal$^+$ cells (from an anterior position defined by the most anterior segment of the clone) in the myotome of RαNLZ2-control-E11.5 has been divided by the number of β-gal$^+$ cells of the clone. This calculation has been done for the contribution of the 32 long clones to segments 1 to 30. The number in the Table corresponds to the mean polyclonal size ± s.e.m.. For short clones, the total number of β-gal$^+$ cells in the corresponding portion of the myotome in RαNLZ2-control-E-11.5 embryos has been divided by the number of β-gal$^+$ cells of the clone. This calculation has been done for the 30 bilateral short clones which altogether contribute to segment 8 to 30. The number of the Table corresponds to the mean polyclonal size ± s.e.m.

Statistical test: we have tested whether the mean polyclonal size of the pool of precursors, calculated from the values of the 30 long and short bilateral clones are different: u=0.517; *P*<0.6. Thus, the mean polyclonal sizes are not statistically different.

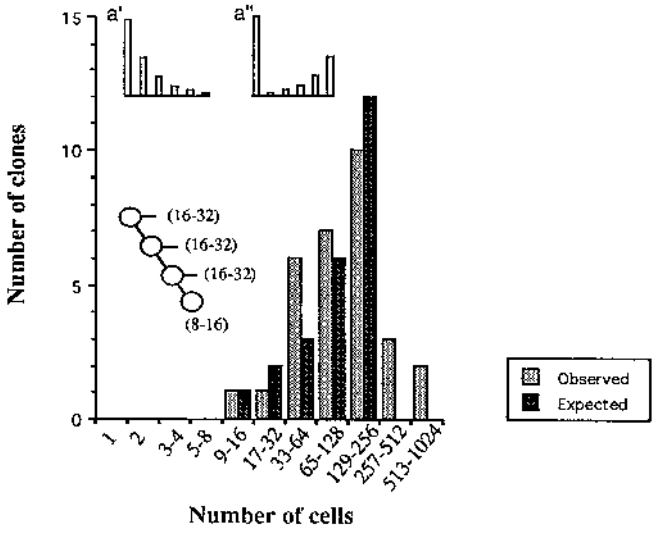

Fig. 7. Number of the long clones in relation to their β-gal$^+$ cell numbers. The x axis represents the number of β-gal$^+$ cells for each class of clones. Classes from left to right in each column group clones with a number of β-gal$^+$ cells double those grouped in the preceeding column. The y axis represents the number of clones. Grey bars represent observed values. Dark bars represent expected numbers following the hypothesis (schematically represented on the left) of production of 256-512 myotomal cells by an asymmetric mode of production of 16-32 β-gal$^+$ cells. Insets: relation between clone frequency and clone size. a′, symmetrical (proliferative) mode; the frequency of clones grouped by exponentially increasing size decreases exponentially. a″, asymmetrical (stem cell) mode; the frequency of clones grouped by exponentially increasing size increases exponentially from a value which corresponds to the limited contribution by one daughter cell of the stem cell progeny. The first column, containing half of the clones, would correspond to short clones (not represented).

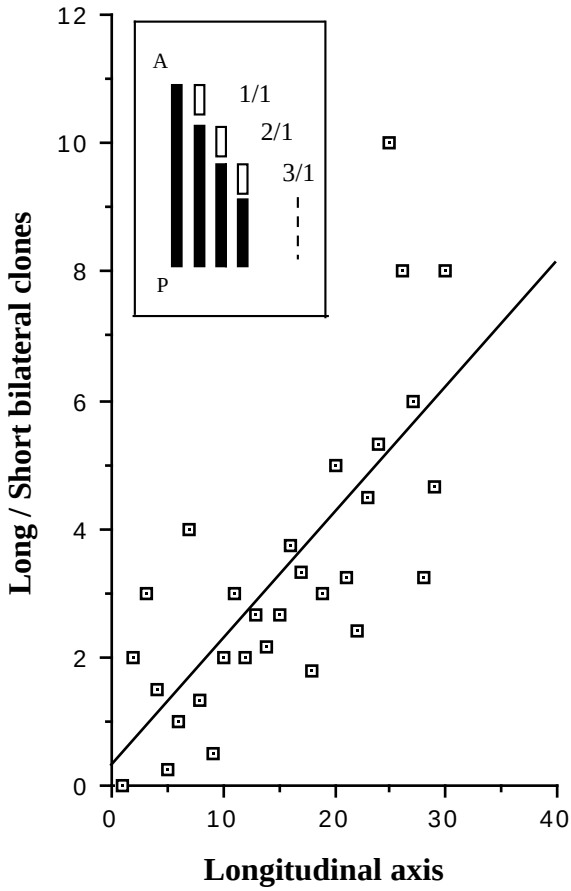

Fig. 8. Increasing overrepresentation of rostrocaudal by L>6 clones. The ratio of the total number of cases when a segment is marked by L>6 clones versus by short bilateral clones (y axis) for each segment (x axis) numbered from the most anterior (1) to the most posterior (30). In the left corner is a schematic representation of the arrangement of small clones in relation to large clones and a theoretical evolution of the factor of over representation as a function of the position along the axis. The slope of the curve indicates the number of segments corresponding to the increase in the ratio of long to short clones. For an increase of 1, the mean size of the small clones produced by a stem cell common to short and long clones, corresponds to 4 segments.

about 100-150 cells (Table 3). The same calculation can be done from the numerical data of short clones. This calculation also shows a pool size of 100-150 (Table 3), and statistical comparison indicates that this value is not different from that obtained from long clones. Therefore, this result is compatible with the hypothesis of a genealogical link between short and long clones. This value of 100-150 cells must only be taken as an indication of precursor pool size since it depends on a comparison between the numbers derived from two different lines of transgenic animals. It should be noted that in addition to an approximation of the pool size, this value provides an indication of the level of cellular organisation in the myotome; indeed, the smaller the polyclonal size, the higher the level of cellular organisation.

From the size of the pool of precursor, it is next possible to calculate the frequency of homologous recombination in the precursor cells. This value derives from total number of precursor cells produced until E11.5, divided by the number of long clones and gives a value of 7.5×10^{-6}. This value is in line with the results obtained from an analysis of *laacZ* recombination frequency from cells in culture (Bonnerot and Nicolas, 1993b). The estimation of 100-150 precursor cells for the myotome is not in contradiction with these recombination values.

DISCUSSION

The method of retrospective clonal analysis used for this study is based on the visualisation of clones whose birth date is randomly fixed by a genetic recombination event that marks a single cell during development (Bonnerot and Nicolas, 1993b; Sanes, 1994; Nicolas, 1995). We have demonstrated here that this method can be applied to the analysis of a mature structure and provides information about events occurring even early during development. Indeed, at E11.5, we detected clones of a large size that originated before the first somite stages, at around day E8 of development (see below). In addition these results illustrate that the method permits an approximation of the time at which precursors of a structure first become arranged into a genealogical coherent pool of cells. Indeed, this is an objective way of defining this first level of cellular organisation as there is no spatial or temporal limitation imposed on

the labelled cells by the marking event. A more general application of this method of random labelling and retrospective analysis may be in helping to define important aspects of early cell behaviour in the cellular systems of organisms whose complete lineage cannot be described because of high cell numbers and periods of variable and unpredictable lineages. Therefore, this method may complement existing prospective methods (Rossant, 1987; Beddington and Lawson, 1990). Furthermore, because this type of analysis requires the examination of a large number of embryos, rather than a unique embryo, it shares the characteristic of prospective methods in that it provides a picture in which events common to all embryos are favoured and putative unique events are underestimated. It is worth noting also that the complete description of a structure will require analysis at several stages during development, because precursor cells at different developmental stages may have different origins.

An important factor in this retrospective analysis is the examination of a sufficiently large sample of clones to give an unbiased description of the mode of development of the structure and clearly this depends on the cellular complexity of the structure (i.e. the number of different clones involved in its production). An indication that the sample size is large enough is the observation that newly produced clones are similar in their characteristics to clones already obtained as this reveals that saturation of the corresponding pool of precursors has been reached. The examination of the clones by their L and Sa values (Figs 3-5) showed that clonal saturation had been reached for both these parameters at L value ≤5 because several clones for each L-value were represented at almost each axial level. The examination of the 32 long clones by their most anterior position (Fig. 6B) showed that ten axial positions were occupied by two or more clones and four positions were occupied by a single clone. Therefore 10 out of 14 axial positions identified by this clonal analysis can be defined by two random events. This indicates that, although we may not have reached a completely saturated picture for this combined characteristic for this category of clones, our sample size is sufficiently large to provide a first understanding of the rules governing myotome formation, particularly with regard to the geometric parameters of clones in relation to their axial position. However, if we next consider the detailed organisation of clones with respect to their longitudinal dimension (for instance, the spacing of cells produced by long clones) none of the clones produced were duplicated. Therefore, the generation of more clones is necessary for an understanding of this aspect of cell behaviour in myotome production.

Finally, it may be important to mention again that the clonal analysis used in this study examines only myotomal cells, therefore it describes only the fraction of progeny of a labelled precursor allocated to the myotome. Consequently, this analysis does not provide any information on the mode of cell division of these precursors, but rather on their combined properties of proliferation and production of a specific cell type. However, a positive consequence of this type of limitation is that it facilitates analyses of cell fate that are difficult to perform by following the mode of cell division and allocation independent of cell type.

Tests of the models

Four major schemes for the formation of longitudinal structures in vertebrates can be envisaged. These models have been schematically presented in the introduction (Fig. 1). Each leads to different expectations concerning the pattern of clones, generated at random during development. In addition, each generates a radically different picture of genealogical history for the precursor cells.

In models based on an early regionalisation of precursor cells (i.e. before axis formation), a pattern of long clones is expected characterised by several non-overlapping classes (Fig. 1B). The longer clones of each class would be uniformly distributed along the axis in a mutually exclusive way. As such, there would be no clonal continuity between cells along the longitudinal axis. Our results are not consistent with this type of model since we observed long clones possessing clonal continuity. In addition, the clones could not be arranged in classes corresponding to mutually exclusive portions of the axis.

In temporal models that postulate axis formation from a pool of changing precursors (i.e. with recruitment of new cells), the excepted pattern of clones excludes very long clones (Fig. 1C). The longest clones would be overlapping and distributed uniformly all along the axis, and there would be no clonal continuity between cells all along the axis. The results of our analysis are not consistent with this model for the same reasons given for the preceding model: the long clones could not be arranged in an overlapping way and were not distributed uniformly along the axis.

In models based on elongation and cell intercalation, a pattern of long clones participating in the formation of the whole axis is expected (Fig. 1A). These clones would originate from cells labelled before intercalation. A second category of shorter clones is expected that corresponds to the descendants of progenitors distributed longitudinally during elongation and intercalation. For these models, there would be two categories of clones (long and short) genealogically related but by a loosely defined link. This is to say that genealogically related cells can be geometrically very distant due to intercalation. All long clones would be produced from a unique pool of cells at the origin of the longitudinal structure; therefore, there would be an apparent clonal continuity for all cells along the axis. Our observations of both long clones and the clonal continuity of cells in all segments are consistent with this model. However, four other characteristics of the clones do not favour this model. (1) The pattern of long clones showed an A-P increase in clonal complexity (Fig. 4B). It is possible to accommodate the elongation-intercalation model with an A-P increase in clonal complexity by postulating a non-uniform distribution of cells during this process. However, in this case, an increase in clonal complexity for small clones is also expected and this was not observed (Fig. 5B). The number of small clones remained the same along the axis. (2) The frequency of long clones was independent of their position along the longitudinal axis and remained uniform (Fig. 6B). An intercalation model favours a class of clones with a maximal longitudinal extension over other classes of clones. (3) The sizes of the long clones were distributed following an asymmetrical mode (Fig. 7). In intercalation models, the pool of precursors of long clones has no self renewal characteristic and therefore the size of the clones does not follow an asymmetric distribution. (4) The pattern of long clones shows an A-P polarity (Fig. 4C). This polarity is not expected with intercalation models because precursor cells randomly labelled (before elongation-intercala-

tion) would show a tendency to be distributed all along the axis. Therefore our results are not consistent overall with an elongation-intercalation model.

In temporal models that postulate axis formation from a pool of permanent progenitors (Fig. 1D), the pattern of clones includes long clones exhibiting polarity. The orientation of the polarity indicates the direction of the temporal evolution of the pool of permanent progenitors. A second category of shorter clones is also expected which corresponds to the descendants of those progenitors deposited along the axis by the permanent pool. Therefore, there are two categories of clones (long and short) genealogically related: long clones are the sisters of corresponding short clones. Because long clones are all produced from a unique pool of cells at the origin of the longitudinal structure, there is clonal continuity between all cells of the axis. The model also predicts that clonal complexity measured as numbers of long clones increases consistently from rostral to caudal and that the size of the clones follows an asymmetric distribution. As indicated above all these predictions are fulfilled by the observations made.

Therefore, the geometric characteristics of clones and their frequencies support the notion that precursor cells of the myotome derive from a pool of cells that self-renews and which follows axis formation during development (Fig. 9).

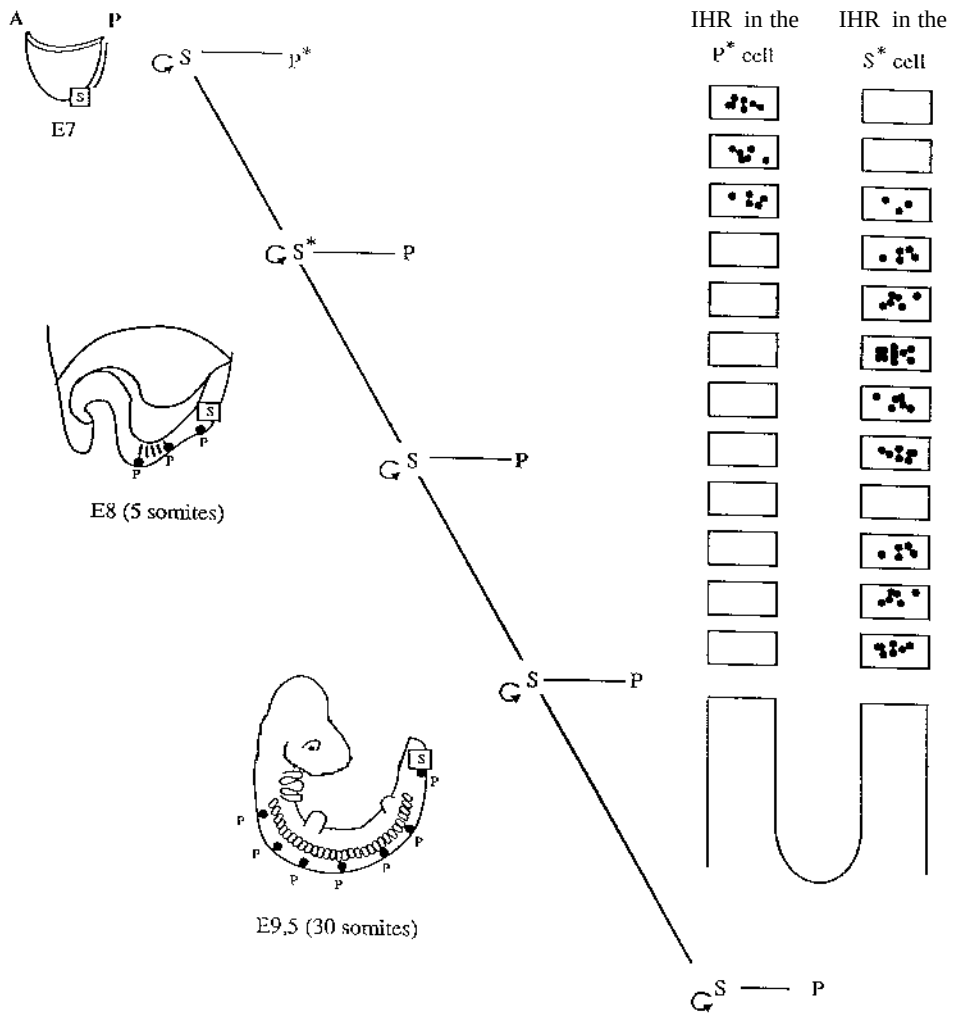

Fig. 9. A model for the production and allocation of the myotomal cells. Analysis of the 153 recombinant clones suggests the following model of allocation and production of myotomal cells. A pool of progenitor cells named S produces cells with two different fates: cells with properties similar to the properties of the mother cells and P cells, which produce myotomal cells and whose lineage is restricted to a few adjacent segments (1 to 6). Their progenies remain clustered but are frequently deposited to both sides of the embryo. The lineage of S cells follows the temporal formation of the embryonic axis from anterior to posterior. S cells are self-renewing. The properties of S cells predict the polarised longitudinal orientation of long clones, and the properties of P cells predict the characteristics of short clones (see the diagram of the paraxial mesoderm on the right). The myotome at E11.5 would be produced by about 100-150 S cells organised in a pool of constant size. The number of P cells increases during the growth of the myotome. It is reasonable to assume that S cells also contribute to compartments outside the myotomal compartment. On the left: lateral views of the embryos and the possible localisation of S cells at E7.5 (late streak stage) and of S and P cells at E8.5 (5 somites stage) and E9.5 (30 somites stage). The pool of S cells is constituted before the bilaterisation of the segmental plate (both clones derived from S and sometimes from P cells, are bilateral). Initial localisation of S cells may be the anterior part of the primitive streak. The pool of S cells remains coherent throughout formation of the paraxial mesoderm and keeps a constant size. S cell descendants are deposited in both left and right in myotomal segments at all axial levels. IHR, intragenic homologous recombination in *laacZ*; the contribution of the clone to only one side of the embryo is represented. Left, a short clone; right, a long clone. The model is based on the following observations. (1) At least part of the myotome is formed by progenitors whose descendants are widely spread throughout the structure (clonal continuity). (2) Clones with a large number of cells demonstrate a longitudinal clonal organisation of the myotome (Fig. 3). (3) This longitudinal organisation of myotome formation is polarised from anterior to posterior as the number of L>6 clones contributing to the segments increases from rostral to caudal (Fig. 4B). (4) There are two categories of clones, long (L>6) and short (L≤ 6) (Fig. 3). (5) The short bilateral clones and long clones have similar mean contributions per segment (Table 2), are derived from pools of progenitor cells of a similar size (polyclonal size of 100-150, Table 3) and located in a structure that includes both right and left segments (Table 1); therefore, it is likely that their pool of precursors is common. (6) The frequency of L>6 clones is constant whatever their SA-value (most anterior axial position) (Fig. 6B) or L value (from 7 to 40, Fig. 6A). Thus, the size of their progenitors pools is the same. (7) The production of precursor cells of long clones is not from a proliferative mode, since the divisions of these precursors produces cells with different potentials for the production of myotomal cells (Fig. 7).

Localisation of the pool of self-renewing cells

What could be the localisation of this pool of precursor cells during embryonic development? A characteristic of long clones is their contribution to both sides of the myotome (Table 1). The progenitor cells of these clones are therefore located in a structure that includes both right and left segments. Moreover, the initial constitution of the precursor pool necessarily precedes the formation of the most rostral part of the myotome and therefore must be present before the formation of paraxial mesoderm. A likely site of localisation is the primitive streak and/or its anterior part at about E8 (Theiler, 1989; Smith et al., 1994). Such an initial localisation suggests that the pool of precursors for long clones is associated with the temporal formation of the paraxial mesoderm at later stages of development. Progenitors would distribute reiteratively into the future segments of paraxial mesoderm during formation of the axis from the primitive streak and then possibly from the tail bud (Gont et al., 1993; Wilson et al., 1995).

Is the paraxial and the axial mesoderm produced by a similar stem cell system?

Prospective analysis of the mouse embryo from the early streak stage to the neural plate stage (Lawson et al., 1991; Lawson and Pedersen, 1992) indicates that paraxial mesoderm, contributing to the most anterior somites, is derived from cells anterior to the primitive streak and these are in accord with results obtained from orthotopic primitive streak grafts (Tam and Beddington, 1987). The descendants of these cells are restricted to a few adjacent somites. Between the late primitive streak stage and the first somite stage, paraxial mesoderm is still formed from the anterior part of the primitive streak and from immediately adjacent epiblast cells. However, it has also been postulated that these regions are formed from newly arising cells that were initially more lateral in the epiblast (Lawson and Pedersen, 1992) and that they contribute to paraxial mesoderm producing 18 somites. Between the early streak stage and the neural plate stage, the anterior portion of the primitive streak produces axial and paraxial mesoderm but the descendants of the initial population are rarely found there; they have been replaced by the descendants of cells from a more lateral position in the embryo.

These results can be compared with our present analysis, which describes progenitor cells for the paraxial mesoderm (corresponding to the most anterior somites), whose descendants are restricted to short groups of adjacent somites. These progenitors may correspond to those at the origin of the short clones described in this study. The data also indicate a continuity in the formation of a certain fraction of paraxial mesoderm from the late primitive streak stage (see also Tam and Beddington, 1987; Tam and Tan, 1992) and this is most evident in the patterns of our most anterior long clones. However, our results further suggest a clonal continuity for the whole paraxial mesoderm. Indeed the clonal continuity of all the cells of the myotome suggests a corresponding clonal continuity for the segment from which the myotome is formed (the somites) and for the structure from which somites are individualised (paraxial mesoderm).

We suggest that, in the mouse, cells contributing to paraxial mesoderm formation, (until at least the 40 somite stage), are organised into a stem cell system constituting a unique, continuous and spatially organised pool. Therefore, cells forming paraxial mesoderm and producing the myotome are not the descendants of a changing population of cells from various regions of the epiblast, primitive streak or node, but rather the descendants of a permanent structure may be constituted at the early streak stage.

This model of myotome formation from paraxial mesoderm may also apply to the axial mesoderm. Distribution of labelled cells in the notochord and node argues that much of the notochord might be formed from a resident population of proliferative cells in the ventral part of the node (Beddington, 1994; Selleck and Stern, 1991, 1992). This hypothesis was based on the finding that groups of cells can populate the entire length of the notochord or the medial part of the somite and that, in some cases, descendants of labelled cells were arranged in a periodic fashion. Although highly suggestive, these findings were not conclusive because periodically spaced contributions from single cells could arise by the elongation and intercalation of cells. Similarly, the population of the entire length of a structure by a group of cells, taken alone, is also compatible with non-stem-cell models. Our results pertaining to the progenitors of the myotome in the mouse exclude these interpretations and support the existence of stem cells in the primitive streak and/or in the node.

Biological significance?

Finally, another implication of these results is that the same pool of precursor cells that maintains a clonal continuity during development of the axis, also contributes the progenitors for the segments that uniformly develop along the axis. In other words, the way that most caudal segments are produced may be the same as for the most rostral segments formed earlier in development. This may suggest a more general ‘permanence’ of axial organiser properties (initially during gastrulation localised in the node and primitive streak) due to the existence of several stem cells pools still present late in development.

However, a possibly important difference between rostral and caudal is that the cellular history of caudal is more complex than rostral. It raises the possibility that some sort of segmental identity in vertebrates is established temporally rather than regionally and raises the question of whether the generation of metameric pattern relies on intrinsic or extrinsic cell behaviour. Selleck and Stern (1992) have also speculated that the medial somite precursor cells in Hensen’s node may be responsible for setting up a metameric pattern in the paraxial mesoderm and that the periodicity of this pattern (also seen after brief heat-shock treatment (Primmett et al., 1988, 1989)) may depend upon a cell autonomous timing mechanism. The issues of whether the temporal control of Hox gene expression in the posterior region (Duboule and Dollé, 1989; Graham et al., 1989) and posterior dominance presiding in anterior-posterior patterning during gastrulation (as described in amphibians; Slack and Tannahill, 1992) relates to the more complex cellular history of caudal remains to be established.

These conclusions share features in common with leech segmentation. Segments in annelids are produced progressively from a step-wise sequence of embryonic cell divisions in teloblasts (Weisblat and Shankland, 1985), with each teloblast establishing a segmental periodicity by an intrinsic mode of stem cell divisions. Moreover, segmental identities of leech blast cells are established through a process of temporal, rather than regional specification (Martindale and Shankland, 1990;

Gleizer and Stent, 1993), and patterns of homeobox gene expression require the stereotyped assembly of blast cell clones, whose segmental identities have been specified at an earlier stage in development, possibly through a series of asymmetric stem cell (teloblasts) divisions (Shankland, 1994). In annelids and chordates, it is possible that what corresponds to the initial asymmetry of the egg in *Drosophila* (necessary for the polarisation and regionalisation of the A-P axis) (Nüsslein-Volhard, 1991) is an asymmetric mode of production of precursors from a pool of stem cells.

We thank Joshua Sanes, Claudio Stern and Nadine Peyreiras for comments on the first version of the manuscript, Joan Shelland for careful reading of this version of the manuscript, Kirstie Lawson for discussions, Suzanne Capgras and Valérie Guyot for excellent technical assistance and members of our laboratory. L. M. thanks M. Kersberg for discussions. This work has been financially supported by the Association Française pour les Myopathies (AFM) and the Association pour la Recherche sur le Cancer (ARC). J. F. N. and C. B. are from the Institut National de la Recherche Medicale.

REFERENCES

Beddington, R. and Lawson, K. A. (1990). Clonal analysis of cell lineages. In *Postimplantation Mammalian Embryos - A Practical Approach.* (ed. J. Cockroft). pp. 267-291. Oxford: Oxford University Press

Beddington, R. S. (1994). Induction of a second neural axis by the mouse node. *Development* **120,** 613-620.

Bonnerot, C., Grimber, G., Briand, P. and Nicolas, J. F. (1990). Patterns of expression of position-dependent integrated transgenes in mouse embryo. *Proc. Natl. Acad. Sci. USA* **87,** 6331-6335.

Bonnerot, C. and Nicolas, J.-F. (1993a). Application of LacZ gene fusions to post-implantation development. In *Methods in Enzymology: Guide to Techniques in Mouse Development*. (ed. P. M. Wassarman and M. L. DePamphilis). pp. 451-469.

Bonnerot, C. and Nicolas, J. F. (1993b). Clonal analysis in the intact mouse embryo by intragenic homologous recombination. *C. R. hebd. Acad. Sci. Paris* **316, 1207-1217.**

Bonnerot, C., Rocancourt, D., Briand, P., Grimber, G. and Nicolas, J. F. (1987). A ß-galactosidase hybrid protein targeted to nuclei as a marker for developmental studies. *Proc. Natl. Acad. Sci. USA* **84,** 6795-6799.

Burke, A. C., Nelson, C. E., Morgan, B. A. and Tabin, C. (1995). *Hox* genes and the evolution of vertebrate axial morphology. *Development* **121,** 333-346.

Christ, B. and Ordahl, C. P. (1995). Early stages of chick somite development. *Anat. Embryol.* **191,** 381-396.

Duboule, D. and Dollé, P. (1989). The structural and functional organization of the murine HOX gene family resembles that of *Drosophila* homeotic genes. *EMBO J.* **8,** 1497-1505.

Gleizer, L. and Stent, G. S. (1993). Developmental origin of segmental identity in the leech mesoderm. *Development* **117,** 177-189.

Gont, L. K., Steinbeisser, H., Blumberg, B. and DeRobertis, E. M. (1993). Tail formation as a continuation of gastrulation: the multiple cell populations of the *Xenopus* tailbud derive from the late blastopore lip. *Development* **119,** 991-1004.

Graham, A., Papalopulu, N. and Krumlauf, R. (1989). The murine and Drosophila homeobox gene complexes have common features of organization and expression. *Cell* **57,** 367-378.

Keller, R. and Danilchik, M. (1988). Regional expression, pattern and timing of convergence and extension during gastrulation of *Xenopus laevis*. *Development* **103,** 193-209.

Keller, R. and Tibbetts, P. (1989). Mediolateral cell intercalation in the dorsal, axial mesoderm of Xenopus laevis. *Dev. Biol.* **131,** 539-49.

Kessel, M. and Gruss, P. (1990). Murine developmental control genes. *Science* **249,** 374-379.

Keynes, R. J. and Stern, C. D. (1988). Mechanisms of vertebrate segmentation. *Development* **103,** 413-429.

Kimmel, C. B., Warga, R. M. and Kane, D. A. (1994). Cell cycles and clonal strings during formation of the zebrafish central nervous system. *Development* **120,** 265-76.

Klarsfeld, A., Bessereau, J.-L., Salmon, A.-M., Triller, A., Babinet, C. and Changeux, J.-P. (1991). An acetylcholine receptor alpha-subunit promoter conferring preferential synaptic expression in muscle of transgenic mice. *EMBO J.* **10,** 625-632.

Lawson, K. A., Meneses, J. J. and Pedersen, R. A. (1991). Clonal analysis of epiblast fate during germ layer formation in the mouse embryo. *Development* **113,** 891-911.

Lawson, K. A. and Pedersen, R. A. (1992). Early mesoderm formation in the mouse embryo. In *Formation and Differentiation of Early Embryonic Mesoderm.* (ed. R. Bellairs). pp. 33-46. New York: Plenum Press.

Lumsden, A. and Keynes, R. (1989). Segmental patterns of neuronal development in the chick hindbrain. *Nature* **337,** 424-428.

Martindale, M. Q. and Shankland, M. (1990). Intrinsic segmental identity of segmental founder cells of the leech embryo. *Nature* **347,** 672-674.

McGinnis, W. and Krumlauf, R. (1992). Homeobox genes and axial patterning. *Cell* **68,** 283-302.

Nicolas, J. F. (1995). Transgene-independent and transgene-dependent reporters in studies on cell lineages and segment-like patterns in the mouse embryo. In *Genes for Development, Cell Growth and Infectious Diseases.* (ed. J. Libbey). pp. 3-15

Nüsslein-Volhard, C. (1991). Determination of the embryonic axes of *Drosophila*. *Development* **1991 Supplement 1,** 1-10.

Primmett, D., Stern, C. and Keynes, R. (1988). Heat shock causes repeated segmental anomalies in the chick embryo. *Development* **104,** 331-339.

Primmett, D. R., Norris, W. E., Carlson, G. J., Keynes, R. J. and Stern, C. D. (1989). Periodic segmental anomalies induced by heat shock in the chick embryo are associated with the cell cycle. *Development* **105,** 119-130.

Puelles, L. and Rubenstein, J. L. R. (1993). Expression patterns of homeobox and other putative regulatory genes in the embryonic mouse forebrain suggest a neuromeric organization. *TINS* **16,** 472-479.

Quinlan, G. A., Williams, E. A., Tan, S. S. and Tam, P. L. (1995). Neuroectodermal fate of epiblast cells in the distal region of the mouse egg cylinder: implication for body plan organization during early embryogenesis. *Development* **121,** 87-98.

Rossant, J. (1984). In *Chimeras in Developmental Biology*. (ed N. Le Douarin and A. McLaren). pp. 89-109. New York: Academic Press.

Rossant, J. (1987). Cell lineage analysis in mammalian embryogenesis. *Curr. Top. Dev. Biol.* **23,** 115-146.

Sanes, J., Rubenstein, J. and Nicolas, J. F. (1986). Use of a recombinant retrovirus to study post-implantation cell lineage in mouse embryos. *EMBO J.* **5,** 3133-3142.

Sanes, J. R. (1994). The laatest in lineaage. *Current Biology* **4,** 1162-1164.

Sanes, J. R., Johnson, Y. R., Kotzbauer, P. T., Mudd, J., Hanley, T., Martinou, J.-C. and Merlie, J. P. (1991). Selective expression of an acetylcholine receptor-lacZ transgene in synaptic nuclei of adult muscle fibers. *Development* **113,** 1181-1191.

Selleck, M. A. and Stern, C. D. (1992). Evidence for stem cells in the mesoderm of Hensen's node and their role in embryonic pattern formation. In *Formation and differentiation of early embryonic mesoderm*. (al., R. B. e., ed), pp. 23-31. New York: Plenum Press.

Selleck, M. A. J. and Stern, C. D. (1991). Fate mapping and cell lineage analysis of Hensen's node in the chick embryo. *Development* **112,** 615-626.

Shankland, M. (1994). Leech segmentation: A molecular perspective. *BioEssays* **16,** 801-808.

Slack, J. M. and Tannahill, D. (1992). Mechanism of anteroposterior axis specification in vertebrates lessons from the amphibians. *Development* **114,** 285-302.

Slack, J. M. W., Holland, P. W. H. and Graham, C. F. (1993). The zootype and the phylotypic stage. *Nature* **361,** 490-492.

Smith, J. L., Gesteland, K. M. and Schoenwolf, G. C. (1994). Prospective fate map of the mouse primitive streak at 7.5 days of gestation. *Dev. Dyn.* **201,** 279-289.

Stern, C. D., Hatada, Y., Selleck, M. A. J. and Storey, K. G. (1992). Relationships between mesoderm induction and the embryonic axes in chick and frog embryos. *Development* **1992 Supplement,** 151-156.

Tam, P. L. and Trainor, P. A. (1994). Specification and segmentation of the paraxial mesoderm. *Anat. Embryol.* **189,** 275-305.

Tam, P. P. L. and Beddington, R. S. P. (1987). The formation of mesodermal tissues in the mouse embryo during gastrulation and early organogenesis. *Development* **99,** 109-126.

Tam, P. P. L. and Tan, S. S. (1992). The somitogenetic potential of cells in the

primitive streak and the tail bud of the organogenesis-stage mouse embryo. *Development* **115,** 703-715.

Theiler, K. (1989). Development and normal stages from fertilization to 4 weeks of age. In *The House Mouse*. Berlin: Springer-Verlag.

Weisblat, D. A. and Shankland, M. (1985). Cell lineage and segmentation in the leech. *Phil. Trans. R. Soc. Lond.* **B312,** 39-56.

Wilson, V., Manson, L., Skarnes, W. C. and Beddington, R. S. (1995). The T gene is necessary for normal mesodermal morphogenetic cell movements during gastrulation. *Development* **121,** 877-886.

(Accepted 17 June 1996)